

# Numerical Investigation of Vesicular Systems and Pion-Nucleus Scattering within the Asynchronous Differential Evolution Method

E.V.Zemlyanaya

*Laboratory of Information Technologies*

*Joint Institute for Nuclear Research, 141980 Dubna, Russia*

Dubna, 20th January, 2017

# Outlines

- Representative case of the helpfulness of the same numerical approach in two very different fields of research.
- Results of studies of two physical systems are presented. For both systems, the basic parameters of the corresponding mathematical models are determined by fitting to experimental data.
- The global minimization of the discrepancy between numerical and experimental parameter values is done within the newly developed method of Asynchronous Differential Evolution
- Information of vesicle systems structure has been obtained the basis of ADE-analysis of small-angle scattering data
- Microscopical analysis of elastic and inelastic pion-nucleus scattering has been done using the ADE-fitting of parameters of pion-nucleon amplitude

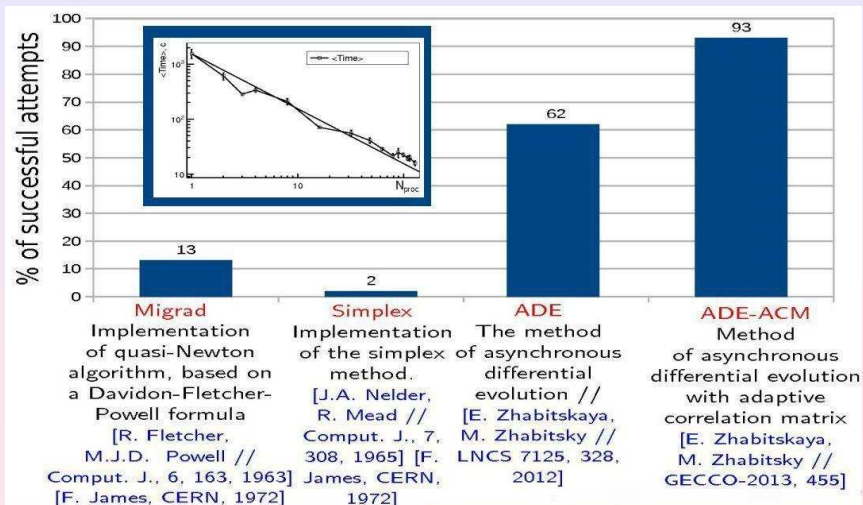
# Coauthors

- E.I.Zhabitskaya, M.A.Kiselev, V.K.Lukyanov, V.L.Aksenov, K.V.Lukyanov, M.V.Zhabitsky  
*Joint Institute for Nuclear Research, Dubna*
- A.Yu.Gruzinov  
*NRC "Kurchatov Institute", Moscow*
- O.M.Ipatova, O.S.Druzhilovskaya  
*Orekhovich Research Institute for Biomedical Chemistry, Moscow*
- I.A.M. Abdul-Magead  
*Cairo University, Egypt*

# Asynchronous Differential Evolution. Why?

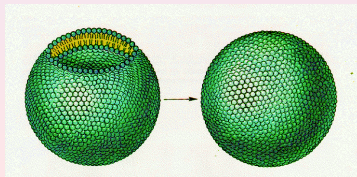
- ADE – stochastic algorithm, one of the most efficient global minimizers [E.Zhabitskaya, M.Zhabitsky // GECCO-2013, 455], based on DE [Price K. V. and Storn, R.V. // J. of Global Opt.-1997]
- ADE is helpful in case the fit function is multi-modal (because the local-search algorithms need a good initial approximation or often failed to find a solution)
- ADE is helpful in case the fit function is time-expensive (because ADE provides an effective parallelism, i.e. saves computer time and a waiting time for a researcher)
- ADE decreases a participation of researcher in the minimization process (because of new adaptive algorithms of automatical tuning of ADE parameters to the features of concrete problem)

# ADE vs other minimizers & effect of parallel implementation



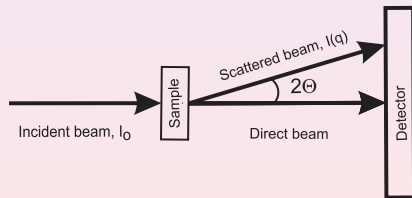
## Phospholipid Vesicles: Motivation

- Information about structure and properties of phospholipid vesicles (liposomes, nanospheres) is important from the viewpoint of practical applications in medicine and pharmacology.
- A study of phospholipid membranes of vesicles allows one to obtain new knowledge about fundamental properties of biological membranes (including Stratum Corneum).
- Recent years, phospholipid delivery nanosystems (PTNS) with an extremely small diameter have been obtained in the V.N.Orekhovich Research Institute of Biomedical Chemistry.



# Why SAXS/SANS? What is SFF?

- Small angle scattering techniques are powerful tools for investigation of structure of nanosystems, including vesicles of phospholipids.
- The separated from factor method (SFF) was developed to obtain information about a structure of vesicular systems from the small angle neutron scattering data (SANS) and the small angle X-ray scattering spectra (SAXS).



# SFF model. I

Within the framework of the SFF model, in the case of the monodispersed vesicle population, the intensity  $I(q)$  is given by the following expression:

$$I_{\text{SFF}}(q) = n I_o F_s(q, R) F_b(q, d), \quad (1)$$

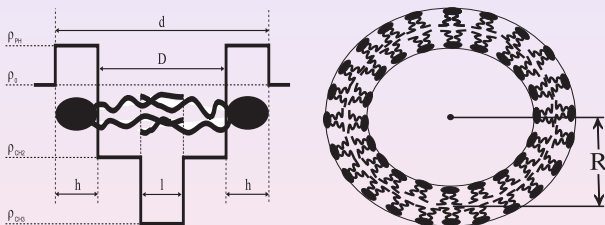
where  $I_o$  is the intensity of the incident beam,  $n$  — a number of vesicles in  $\text{cm}^3$ ,  $F_s(q, R)$  — form factor of the spherical surface with radius  $R$ ,  $F_b(q, d)$  — form factor of the symmetric lipid bilayer,  $d$  — thickness of the lipid bilayer of ULVs.  $F_s(q, R)$  and  $F_b(q, d)$  are determined as follows:

$$F_s(q, R) = \left( 4\pi R^2 \frac{\sin(qR)}{qR} \right)^2, \quad F_b(q, \Theta_b) = \left( \int_{-d/2}^{+d/2} \rho_c(x) \cos(qx) dx \right)^2$$



## SFF model. II

Here  $\rho_c(x)$  is a contrast between the scattering length density of the lipid bilayer and the density of the solvent.



The “step” form is the representative example of the density distribution across bilayer. Here  $\rho_0$  is the density of the solvent,  $\rho_{CH2}$  — density of the hydrocarbon chains,  $\rho_{PH}$  — density of polar head region.

## SFF model. III

Polydispersity  $\sigma$  of the the average radius is accounted utilizing the Schulz distribution with coefficient  $m$ :

$$G(\tilde{R}, R) = \frac{\tilde{R}^m}{m!} \left(\frac{m+1}{R}\right)^{m+1} \exp\left[-\frac{(m+1)\tilde{R}}{R}\right], \quad \sigma = \frac{1}{\sqrt{m+1}}$$

The intensity  $I_m$  for the polydispersed system is obtained by means of a standard convolution procedure.

$$I_m(q) = \frac{\int_{R_{\min}}^{R_{\max}} I_{SFF}(q, \tilde{R}) G(\tilde{R}, R) d\tilde{R}}{\int_{R_{\min}}^{R_{\max}} G(\tilde{R}, R) d\tilde{R}}.$$

## SFF model. IV

The final expression of intensity  $I(q)$  has the following form:

$$I(q) = I_m(q) + \frac{1}{2} \Delta^2 \frac{d^2 I_m(q)}{dq^2} + I_B, \quad (2)$$

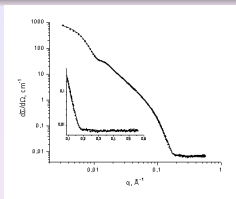
$I_B$  – parameter of incoherent background,  $\Delta^2$  – 2<sup>nd</sup> momentum of a resolution spectrometer function.

A discrepancy between theoretical and experimental values of intensity ( $N$  – number of experimental points;  $k$  – number of fitted parameters):

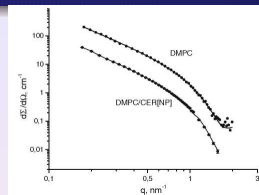
$$R_N = \frac{1}{N - k} \sum_{j=1}^N \left( \frac{I(q_j) - I^{\text{exper}}(q_j)}{\delta^{\text{exper}}(q_j)} \right)^2. \quad (3)$$

Fitting procedure: (1) the standard least square method;  
(2) ADE global minimization algorithm.

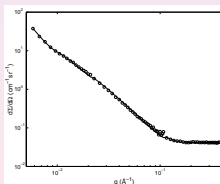
# SFF analysis of SANS data: earlier results, without ADE



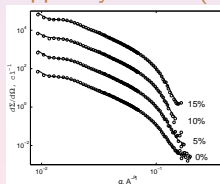
DMPC ULVs (PSI)  
EuroBioPhys J **35** 6 (2006) 477-493



DMPC (YuMO),  
Ceramide-3 ("Yellow Submarine")  
Appl Phys A **116** (2014) 319-325



Ceramide-6 ("Yellow Submarine")  
Crystallography Rep. **51** (2006) S22-S26

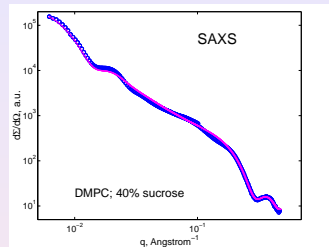
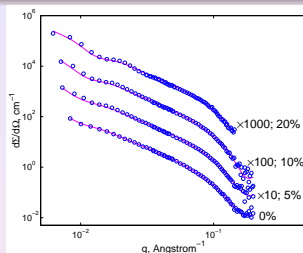


DPPC/DMSO/D<sub>2</sub>O (YuMO)  
Crystallography Rep (2017) in press

## SANS & SAXS: recent results

- A structure of polydispersed population of DMPC unilamellar vesicles in sucrose solutions have been studied in dependence of the sucrose concentration in H<sub>2</sub>O (D<sub>2</sub>O). Basic parameters of vesicular system are fitted to SANS spectra for sucrose concentration 0% - 20% and to SAXS data in the case of 40% concentration.
- SANS spectra were measured on YuMO small-angle spectrometer of IBR-2 reactor (JINR, Dubna, Russia). SAXS measurements were performed on the A2 system of the Doris III synchrotron source (DESY, Hamburg, Germany).
- Then our SFF-ADE approach has been employed to the analysis of PTNS nanoparticles on the basis of SAXS data measured on the DICS1 station (National Research Centre “Kurchatov Institute”, Moscow)

# DMPC: SANS (YuMO) and SAXS (Doris III)



SANS: least square method (subroutine DFUMIL from JINRLIB);

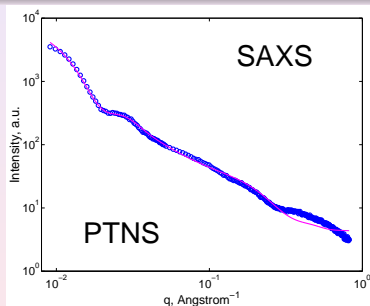
SAXS: ADE-ACM

Crystallography Rep **60** 1 (2015) 143-147

Sucrose	R, Å	d, Å	D, Å	$\sigma$ , %	$\chi^2$
0%	307.5±5	49.8±1	16.5±1.7	30	1.1
5%	270.6±5	48.1±2	19.9±2.9	31	5.9
10%	243.4±3	47.6±1	23.0±3.0	27	6.6
20%	213.4±2	44.5±2	25.1±2.8	26	9.1
40%	190.6±2	34.8±1	27.2±2.8	26	1.7

# SAXS spectrum: 25% (w/w) PTNS in water

PTNS sample was prepared via dilution of lyophilized PTNS (25% w/w) in water. The SAXS spectrum was measured at the DICSI station of the Kurchatov Synchrotron Radiation Source (Moscow)

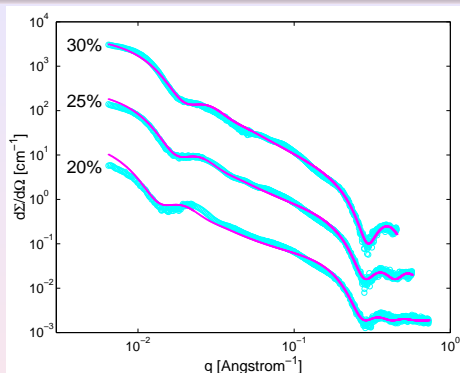


J. Phys. CS 724 (2016) 012056

SFF:  $R = 135.4 \pm 2 \text{ \AA}$ ;  $d = 43.5 \pm 1 \text{ \AA}$ ;  $\sigma = 27 \%$ ;  $\chi^2 = 2.6$

HS:  $R = 135.4 \pm 1 \text{ \AA}$ ;  $d = 36.9 \pm 1 \text{ \AA}$ ;  $\sigma = 33 \%$ ;  $\chi^2 = 3.5$

# PTNS; 20–30% concentration of maltose in water



Concentration	$R, \text{ \AA}$	$d, \text{ \AA}$	$D, \text{ \AA}$	$\chi^2$	$\sigma,$
20%	$205 \pm 3$	$44.8 \pm 0.4$	$27.1 \pm 0.2$	1.1	23
25%	$160 \pm 2$	$39.9 \pm 0.3$	$26.2 \pm 0.2$	0.9	23
30%	$141 \pm 2$	$37.0 \pm 0.3$	$22.6 \pm 0.2$	1.2	24



## Pion-nucleus scattering: motivation and aim

In theoretical study of  $\pi$ -nucleus scattering, two approaches are usually employed:

First, microscopic local transformed Kisslinger potential having six fitted parameters. It is based on  $s$ - and  $p$ -  $\pi N$  scattering amplitudes and respective density distribution function of nuclei.

Second, the Glauber high-energy approximation for the  $\pi$ -nucleus amplitude that uses analytic form of the  $\pi N$  amplitude and the nuclear density is integrated along the *straight line* trajectory of scattering.

We utilize the HEA  $\pi$ -nucleus microscopic OP and apply it by solving the relativistic wave equation Our aim: explanation of experimental data on both elastic and inelastic scattering in the region of  $\pi N$  (3 3)-resonance energies and estimation of the “in-medium” effect on the elementary  $\pi$ -nucleon amplitude.



## How and what we deal with elastic scattering case

- The OP depends on the  $\pi N$  amplitude which itself depends on three parameters [Phys. At. Nucl. **73** (2010) 1443] obtained by fitting the calculated  $\pi A$  cross sections to the respective experimental data on *elastic* scattering
  - $\sigma$ , total cross section
  - $\alpha$ , the ratio of real to imaginary part of the forward  $\pi N$  amplitude
  - $\beta$ , the slope parameter
- The established best-fit “in-medium”  $\pi N$  parameters are compared with the corresponding parameters of the “free”  $\pi N$  scattering amplitudes [Phys. At. Nucl. **77** (2014) 100]
- Application have been made for elastic scattering of pions on nuclei  $^{28}\text{Si}$ ,  $^{58}\text{Ni}$ ,  $^{40}\text{Ca}$  and  $^{208}\text{Pb}$  at energies 130–291 MeV.
- 291 MeV: “standard” minimization; other energies: ADE.

## How and what we deal with inelastic scattering case

- By using the same method, we substitute into the microscopic OP the generalized density distribution function  $\rho(r, \xi)$  depended on the collective variables  $\xi$  of a target nucleus, and thus obtain the microscopic *transition* OP (TOP)  $U_{inel}(\mathbf{r}, \xi)$  responsible for inelastic scattering with excitations of the nuclear collective states<sup>1</sup>.
- This TOP provides calculations of the pion-nucleus inelastic scattering with excitations of the quadruple  $2^+$  and octuple  $3^-$  collective states of the nuclei  $^{28}\text{Si}$ ,  $^{58}\text{Ni}$ ,  $^{40}\text{Ca}$  and  $^{208}\text{Pb}$  studied earlier in elastic scattering of pions.
- The best-fit “in-medium”  $\pi N$  parameters are used for analysis of *inelastic* scattering data. This scheme does not contain free parameters except the static (or dynamic) deformations of nuclei  $\beta_\lambda$  ( $\lambda = 2, 3$ ) that characterize their excited states.

<sup>1</sup>Intern. J. Mod. Phys. E 24 (2015) 1550035

## Elastic scattering: basic equations

The cross sections are calculated by solving the Klein-Gordon equation in its form at conditions  $E \gg U$

$$(\Delta + k^2) \psi(\vec{r}) = 2\bar{\mu}U(r)\psi(\vec{r}), \quad U(r) = U^H(r) + U_C(r)$$

Here  $k$  is relativistic momentum of pions in c.m. system,

$$k = \frac{M_A k^{\text{lab}}}{\sqrt{(M_A + m_\pi)^2 + 2M_A T^{\text{lab}}}}, \quad k^{\text{lab}} = \sqrt{T^{\text{lab}} (T^{\text{lab}} + 2m_\pi)},$$

and  $\bar{\mu} = \frac{EM_A}{E + M_A}$  – relativistic reduced mass,  $E = \sqrt{k^2 + m_\pi^2}$  – total energy,  $m_\pi$  and  $M_A$  – the pion and nucleus masses.

# Microscopic optical potential

HEA-based microscopic OP:

$$U^H = -\sigma(\alpha + i) \cdot \frac{\hbar c \beta_c}{(2\pi)^2} \int_0^\infty dq q^2 j_0(qr) \rho(q) f_\pi(q),$$

where

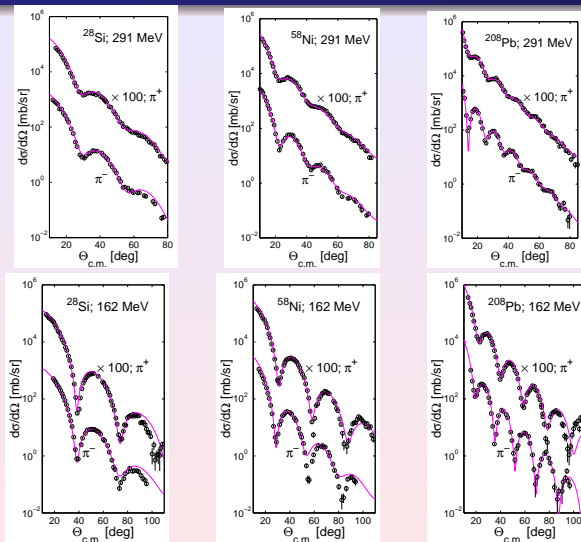
$f_\pi(q) = \exp\left[\frac{-\beta q^2}{2}\right]$  – formfactor of  $\pi N$ -scattering amplitude;  
 $\beta_c = k/E$ ;  $\rho(q)$  – formfactor of the nuclear density distribution.

Symmetrized Fermi-function is used for nuclear density distribution:

$$\rho_{SF}(r) = \rho_0 \frac{\sinh(R/a)}{\cosh(R/a) + \cosh(r/a)}, \quad \rho_0 = \frac{A}{1.25\pi R^3} \left[1 + \left(\frac{\pi a}{R}\right)^2\right]^{-1}$$

Parameters of radius  $R$  and diffuseness  $a$  are known from electron-nucleus scattering.

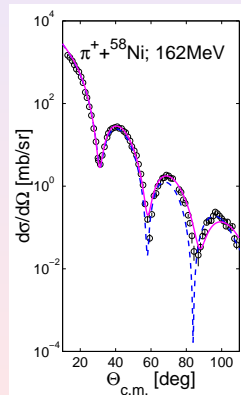
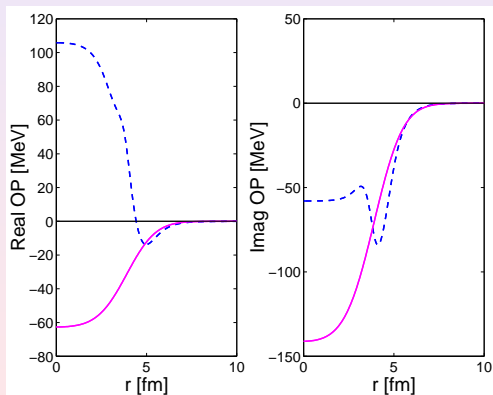
# $\pi^\pm$ -nucleus elastic scattering: $T_{lab}=162$ and 291 MeV



# Comparison with Kisslinger-type OP: $\pi^+ + {}^{58}\text{Ni}$ at 162 MeV

Solid: 3-parameter microscopic OP

Dashed: Kisslinger potential from M.B.Johnson and G.R.Satchler,  
Annals of Phys. 248 (1996) 134







## Generalization to inelastic scattering case: density

We transform the form factor of a spherically-symmetric density distribution function

$$\rho(\mathbf{q}) = \int e^{i\mathbf{q}\mathbf{r}} \rho(r) d^3r$$

by using the following standard prescription:

$$\mathbf{r} \Rightarrow r + \delta^{(\lambda)}(\mathbf{r}), \quad \delta^{(\lambda)}(\mathbf{r}) = -r \left(\frac{r}{R}\right)^{\lambda-2} \sum_{\mu} \alpha_{\lambda\mu} Y_{\lambda\mu}(\hat{r}),$$

where  $\alpha_{\lambda\mu}$  – the nuclear deformation collective motion variables for  $\lambda=2,3$ . Substituting this one in the density and terminating their expansions at linear terms in  $\delta^{(\lambda)}(\mathbf{r})$  one obtains

$$\rho(\mathbf{r}) = \rho(r) + \rho_{\lambda}(r) \sum_{\mu} \alpha_{\lambda\mu} Y_{\lambda\mu}(\hat{r}), \quad \rho_{\lambda}(r) = -r \left(\frac{r}{R}\right)^{\lambda-2} \frac{d\rho(r)}{dr}$$

## Generalization to inelastic scattering case: TOP

Then one gets their form factors

$$\rho(\mathbf{q}) = \rho(q) + \rho_\lambda(q) i^\lambda \sum_\mu \alpha_{\lambda\mu} Y_{\lambda\mu}(\hat{\mathbf{q}})$$

$$\rho(q) = 4\pi \int j_0(qr) \rho(r) r^2 dr, \quad \rho_\lambda(q) = 4\pi \int j_\lambda(qr) \rho_\lambda(r) r^2 dr$$

Finally, we obtain potentials for elastic and inelastic scattering<sup>a</sup>

$$U(\mathbf{r}) = U_{opt}(\mathbf{r}) + U^{(\lambda)}(\mathbf{r}), \quad U^{(\lambda)}(\mathbf{r}) = U_\lambda(r) \sum_\mu \alpha_{\lambda\mu} Y_{\lambda\mu}(\hat{\mathbf{r}}),$$

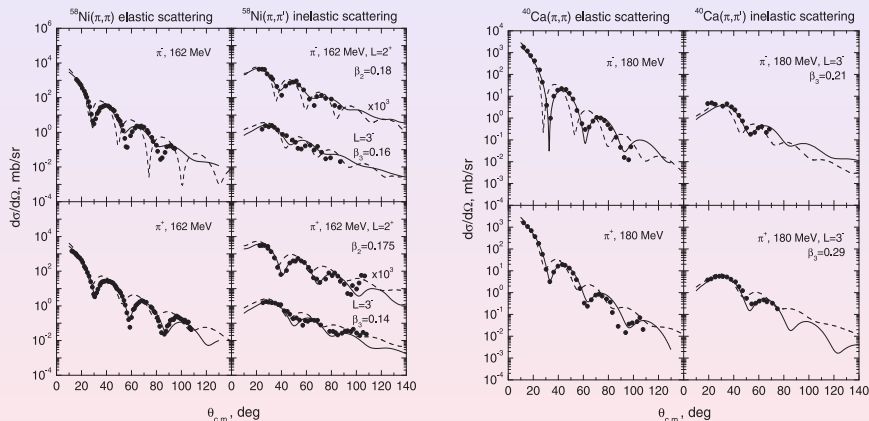
$$U_{opt}(r) = -\frac{(\hbar c)\beta_c}{(2\pi)^2} \sigma (\alpha + i) \int j_0(qr) \rho(q) f(q) q^2 dq,$$

$$U_\lambda(r) = -\frac{(\hbar c)\beta_c}{(2\pi)^2} \sigma (\alpha + i) \int j_\lambda(qr) \rho_\lambda(q) f(q) q^2 dq.$$

---

<sup>a</sup>The spherically symmetric  $U_{opt}(r)$  provides elastic scattering calcs;  $U_\lambda(r)$  – the transition OP (TOP) for of inelastic scattering cross sections calcs with excitations of  $2^+$  and  $3^-$  collective states of nuclei

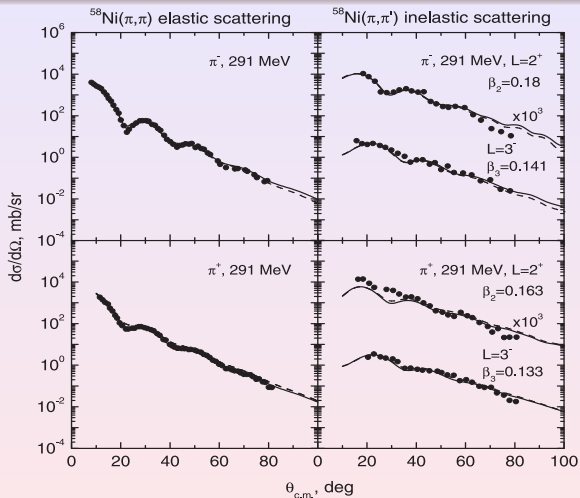
# Elastic and inelastic scattering



solid – “in-medium”, dashed – free  $\pi N$  scattering parameters

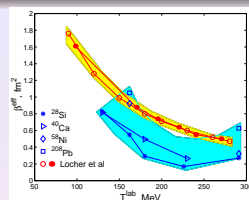
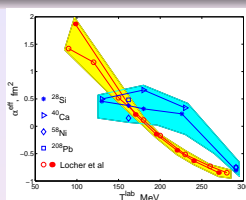
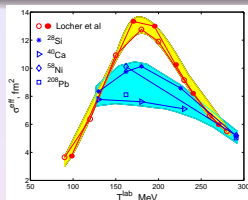


# Elastic and inelastic scattering for $\pi^\pm + {}^{58}\text{Ni}$ at 291 MeV

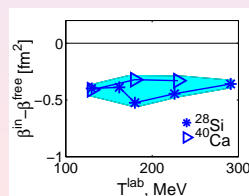
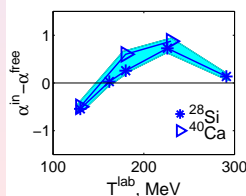
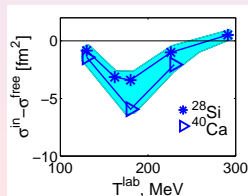


solid – “in-medium”, dashed – free  $\pi N$  scattering parameters

# In-medium effect on $\pi N$ scattering



- Yellow: “free”  $\pi^\pm N$  parameters Nucl. Phys. B 27 (1971) 593
- Blue: the best fit values  $X^{eff} = (X_{\pi^+} + X_{\pi^-})/2$ ;  $X = \sigma, \alpha, \beta$
- Maximum of bell-like forms of  $\sigma^{free}$  and  $\sigma^{eff}(T^{lab})$  at the same  $T^{lab}$
- “Blue” and “yellow” regions become closer at  $T^{lab} > 250$  MeV.



# Summary

- The ADE-based global minimization allowed to successfully investigate two multi-parameter physical systems and to obtain new results.
- The SFF method has been employed for analysis of SAXS spectra from polydispersed PTNS system. Comparison of DMPC and PTNS spectra allowed to make conclusion about the vesicular structure of the PTNS. Estimations of basic parameters of PTNS vesicles have been made.
- HEA-based 3-parametric micro-OP has been shown to provide a reasonable agreement with experimental data on  $\pi^\pm$ -nucleus elastic and inelastic scattering at energies 130–290 MeV. The proposed scheme for inelastic scattering operates with the primary nature of a target nucleus: *the density distribution function*. The theoretical approach is shown to be appropriate to study in-medium effect on the process of  $\pi N$  scattering.

Thank you  
for your attention!